Brief Communications

Lateralized Odor Preference Training in Rat Pups Reveals an Enhanced Network Response in Anterior Piriform Cortex to Olfactory Input That Parallels Extended Memory

Christine J. Fontaine,[1,2] Carolyn W. Harley,[2] and Qi Yuan[1]

[1]Biomedical Sciences, Faculty of Medicine, and [2]Department of Psychology, Faculty of Science, Memorial University of Newfoundland, St. John's, Newfoundland, Canada, A1B 3V6

The present study examines synaptic plasticity in the anterior piriform cortex (aPC) using *ex vivo* slices from rat pups given lateralized odor preference training. In the early odor preference learning model, a brief 10 min training session yields 24 h memory, while four daily sessions yield 48 h memory. Odor preference memory can be lateralized through naris occlusion as the anterior commissure is not yet functional. AMPA receptor-mediated postsynaptic responses in the aPC to lateral olfactory tract input, shown to be enhanced at 24 h, are no longer enhanced 48 h after a single training session. Following four spaced lateralized trials, the AMPA receptor-mediated fEPSP is enhanced in the trained aPC at 48 h. Calcium imaging of aPC pyramidal cells within 48 h revealed decreased firing thresholds in the pyramidal cell network. Thus multiday odor preference training induced increased odor input responsiveness in previously weakly activated aPC cells. These results support the hypothesis that increased synaptic strength in olfactory input networks mediates odor preference memory. The increase in aPC network activation parallels behavioral memory.

Introduction

Efforts to assess sustained increases in the AMPA receptor (AMPAR)-mediated excitation predicted to support cortical memory are typically not successful, although initial increases have been documented (Whitlock et al., 2006; Matsuo et al., 2008). It is widely assumed that increases in AMPAR strength are fundamental underpinnings of memory (Malenka and Bear, 2004). We suggest one difficulty in demonstrating sustained increases in AMPAR strength relates to problems of identifying relevant pathways and controlling individual subject variability.

Here we use lateralized early odor preference learning in the rat pup as a powerful model for assessing the contribution of increases in AMPAR strength to the maintenance of a cortical memory. We also take advantage of the model to examine changes in cortical network representations using calcium imaging.

The anterior piriform cortex (aPC) was shown to be recruited in early odor preference learning by Sullivan and colleagues (Roth and Sullivan, 2005; Raineki et al., 2009). We have demonstrated that blocking NMDAR or β-adrenoceptors in the aPC during training prevents odor preference memory (Morrison et al., 2013). We also showed that, following one-trial training, the AMPAR-mediated field EPSP (fEPSP) from the lateral olfactory tract (LOT) synapses in the aPC of trained rat pups was enhanced at 24 h, the time of memory expression.

Now we investigate the relationship between increases in AMPAR input in the aPC and memory expression using varying memory durations. The preference memory duration is readily varied in this model. A single 10 min trial pairing odor and maternal care stimuli in the first week of life produces an odor preference at 24 h that is not seen at 48 h. Manipulations that extend learning-associated intracellular signaling in the olfactory bulb (Christie-Fougere et al., 2009; McLean et al., 2009) or that increase the frequency of odor and reward pairings (Woo and Leon, 1987) produce memories of varying durations, including robust life-long memory (Fillion and Blass, 1986). We therefore ask whether the previously observed increase in AMPAR responses in the aPC following a single training trial would disappear at 48 h and whether extending memory using multiple training trials would prolong the AMPAR-mediated enhanced fEPSP to 48 h.

Until postnatal day 11 (PD11) in rats, odor input is lateralized to both the olfactory bulb and the olfactory cortex, due to lack of anterior commissural projections (Schwob and Price, 1984; Kucharski and Hall, 1987, 1988). Thus, each rat pup is its own control for memory and physiology. This has permitted us to identify sustained memory-related cortical changes.

Materials and Methods

Subjects

Sprague Dawley rat (Charles River) pups of either sex were used. Litters were culled to 12 on PD1 (birth being PD0). The dams were maintained on a 12 h light/dark cycle with *ad libitum* food and water. Experimental

Received June 13, 2013; revised July 31, 2013; accepted Aug. 14, 2013.

Author contributions: C.J.F., C.W.H., and Q.Y. designed research; C.J.F. and Q.Y. performed research; C.J.F. and Q.Y. analyzed data; C.J.F., C.W.H., and Q.Y. wrote the paper.

This work was supported by a CIHR operating grant (MOP-102624) to Q.Y. We thank Amin Shakhawat and Dr. Qinlong Hou for technical assistance.

The authors declare no competing financial interests.

Correspondence should be addressed to Dr. Qi Yuan, Division of Biomedical Sciences, Faculty of Medicine, Memorial University, St. John's, NL, Canada, A1B 3V6. E-mail: qi.yuan@med.mun.ca.

DOI:10.1523/JNEUROSCI.2503-13.2013

 0270-6474/13/3315126-06$15.00/0

procedures were approved by Memorial University's Institutional Animal Care Committee.

Behavioral training and testing

General protocol. Animals underwent odor conditioning to peppermint-scented bedding (Morrison et al., 2013). Animals were removed from the dam and placed on unscented bedding for 5 min before training. Pups were randomly assigned to experimental [odor plus stroking (O/S^+)] and control [odor without stroking (O/S^-)] conditions. Pups in the O/S^+ group were placed on peppermint-scented bedding (0.3 ml peppermint/500 ml bedding) and stroked with a small paintbrush for 30 s every 30 s over 10 min. O/S^- pups were placed on scented bedding for 10 min without stroking. The 1 d training occurred on PD6. Multiday training was conducted on PD3–PD6. A two-choice odor preference test was given either 24 or 48 h following the final training session.

The testing apparatus consisted of a stainless steel cage (30 × 20 × 18 cm) on top of two training boxes separated by a 2 cm neutral zone. One box contained peppermint-scented bedding and the other contained unscented bedding. Testing began when a pup was placed in the neutral zone. The time the pup spent over each box was recorded for five 1 min trials. Between trials, pups had 1 min of rest in an unscented cage. The percentage of time spent over the peppermint bedding was calculated.

Lateralized learning and memory. A single naris occlusion protocol was used to test whether lateralized learning that is confined to the spared hemisphere (Yuan and Harley, 2012) can be induced by multitrial training. O/S^+ and O/S^- multiday behavioral training was performed in pups from PD3–PD6 as described above. During training, all animals received left naris occlusion for each session. Nose plugs were constructed from polyethelyne-20 tubing (Cummings et al., 1997). Pups were removed from the dam, a small dab of a sterile 2% xylocaine gel was placed on the left naris, and they were given a 1 min rest before gentle plug insertion. Pups were left resting for 5 min before subsequently subjected to either O/S^+ or O/S^- training. Pups were tested 48 h following the final training day (see Fig. 2*A*). They were first tested with the left naris occluded with odorless silicone grease, which caused no pain or disturbance in pups and was applied repeatedly between trials if necessary. Immediately following testing, the left naris was cleaned and a plastic noseplug was inserted into the right naris. The animal was then given 10 min of rest before testing with the right naris occluded.

pCREB immunohistochemistry

To ascertain that odor information is restricted to the spared hemisphere during naris occlusion, and that repeated naris occlusions did not visibly damage the physical structure or reactivity of neurons in the olfactory bulb or aPC, slice immunohistochemistry was performed using pCREB (1:100; Cell Signaling Technology). To test functional blockage during naris occlusion, animals were given single naris occlusion, then returned to the dam for 20–30 min before being exposed to peppermint oil on tissue paper for 10 min. Animals were then anesthetized by chloral hydrate (400 mg/kg i.p.) and perfused with 4% paraformaldehyde dissolved in PBS. To test the effect of reversible naris occlusions on tissue, multitrial animals underwent 15 min single naris occlusions on PD3-PD6, followed by a 48 h rest. Animals were then exposed to peppermint oil for 10 min before perfusion. The brains were postfixed in paraformaldehyde and then transferred to a 20% sucrose solution for 24 h. Brain slices were collected using a cryostat. Immunohistochemistry was performed as previously described (Morrison et al., 2013). Alternate slices were collected for Nissl staining.

Activation was quantified using region of interest (ROI) image analyses on a Bioquant system (Morrison et al., 2013). The relative optical densities (ROD) of the mitral cell layer in the midlateral region of the olfactory bulb and of the pyramidal cell layer in the lateral aPC were compared according to the formula ROD = |(OD of ROI − OD of background)/OD of background|. Spared hemispheres were compared with the occluded hemispheres.

Ex vivo *slice electrophysiology*

We tested synaptic changes in aPC brain slices harvested at ~48 h following odor conditioning. Pups undergoing *ex vivo* electrophysiology received either 1 d (O/S^+) or 4 d odor training (O/S^+ or O/S^-) with one naris occluded by a plastic plug 5 min before training and removed immediately after.

Pups were euthanized 48 h following final training and brain slices prepared. All pups were trained and killed before PD10 to ensure lateralized learning (Kucharski and Hall, 1987, 1988). Pups were anesthetized using halothane and decapitated. Sagittal PC slices (400 μm) were cut on a vibratome into a cutting solution (in mM: 83 NaCl, 2.5 KCl, 3.3 $MgSO_4$, 1 NaH_2PO_4, 26.2 $NaHCO_3$, 22 glucose, 72 sucrose, 0.5 $CaCl_2$) equilibrated with 95% O_2/5% CO_2 (Apicella et al., 2010; Morrison et al., 2013), then incubated in the same solution at 34°C for 30 min before being left at room temperature. Slices were transferred to an open bath recording chamber continuously perfused with artificial CSF (aCSF; in mM: 110 NaCl, 2.5 KCl, 1.3 $MgSO_4$, 1 NaH_2PO_4, 26.2 $NaHCO_3$, 22 glucose, 2.5 $CaCl_2$) heated to 30.0–32.0°C. Slices were visualized with an Olympus BX51WI upright microscope. A concentric bipolar stimulating electrode (FHC) was placed in LOT of the aPC, and a glass recording pipette filled with aCSF was placed in layer Ia. Data acquisition used a multiclamp 700B amplifier (filtered at 2 kHz and digitized at 10 kHz) and pClamp10 software.

A stimulation profile of fEPSPs was recorded. Stimulation intensities increased from 10 to 60 μA. Five sweeps were recorded at each intensity (separated by 20 s). Following the stimulation profile, a paired-pulse protocol (two consecutive stimulations with an interval of 50 ms) was recorded using midrange stimulation. The procedure was repeated with the corresponding slice from the opposite hemisphere.

Electrophysiology data were analyzed offline using Clampfit and Igor softwares. The size of the presynaptic volley at each intensity was plotted against the slope of the corresponding fEPSP to construct input/output (I/O) curves. Pharmacological studies have shown that the slope of the fEPSP we measured is largely mediated by AMPAR (Franks and Isaacson, 2005; Morrison et al., 2013). The average I/O slopes of occluded and spared hemispheres were compared. Paired-pulse recordings were analyzed by comparing the slope of the second fEPSP to the first to obtain a paired-pulse ratio (PPR).

Calcium imaging

To assess the influence of the training-induced increase in synaptic response on overall firing patterns in the aPC, ensembles of pyramidal cells were visualized by imaging PC slices bulk-loaded with the calcium indicator dye Oregon Green-1 AM. Action potentials in dye-loaded cells generate somatic calcium transients that identify cells recruited by LOT stimulation (Apicella et al., 2010). Activity maps of recruited cells were created by averaging the peak ΔF/F images collected from several consecutive stimulus trials (see Fig. 4*A*).

For *ex vivo* population calcium imaging (Apicella et al., 2010; Yuan et al., 2011), brain slices were harvested from pups with single naris occlusion within 48 h following multiday training. Slices were incubated in aCSF containing Oregon Green BAPTA-1 AM (10–20 μM, with 0.02% Pluronic F-127; Invitrogen) at 34°C for 30–60 min, before transferring to aCSF only at room temperature. Slices were allowed to recover for at least 30 min before imaging. Image acquisition (488 nm excitation, 2 × 2 binning, 20 Hz) was performed with a cooled-CCD camera system (T.I.L.L. Photonics). Image processing and analysis were performed with ImageJ (NIH). The LOT layer was stimulated with a concentric bipolar stimulation electrode at 10–50 μA. Activity maps of cell ensembles were constructed from five stimulus trials. All images from an individual experiment were processed identically. The first three or four image frames (~200 ms) following the stimulus were averaged to generate the peak dF/F signal for individual trials. Individual peak dF/F images were then averaged to represent the cell ensembles activated by LOT stimulation. The resulting peak dF/F images were bandpass filtered (to reduce diffuse signals) and processed using a template-based detection with criteria based on cell size (~20 μm diameter) and intensity (>50% background) according to previously established protocols (Apicella et al., 2010; Yuan et al., 2011). Detected cells from the correlation maps were counted automatically and the correlation maps were masked to reveal the binary cell ensembles activated (see Fig. 4*A*).

The I/O relationship was constructed by measuring the percentage of the total activated cells at each stimulation intensity. Total activated cells

were defined as the maximum cells activated—normally by the highest stimulation intensity used (50 μA), but in some cases, the activated cells were saturated at lower stimulation intensities. The I/O relationships were fitted with sigmoid curves and the stimulation intensities for activating half of the maximum cells (X_{half}) were compared in the spared versus occluded hemispheres.

Statistical analyses

Statistical analyses were performed using OriginPro software. One-way ANOVAs were used for behavioral tests in Figure 1. Fischer LSD *post hoc* comparisons were used to evaluate differences between behavioral groups. Paired *t tests* evaluated intra-animal two-group comparisons for behavioral, electrophysiological, and calcium imaging data (Fig. 2, 3, 4).

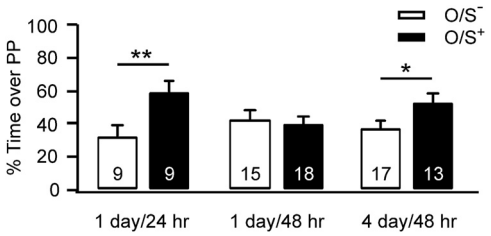

Figure 1. Early odor preference memory is extended to 48 h by multiday training. Bars show percentage of time spent over peppermint-scented bedding in a two-choice test. $^{**}p < 0.01$, $^{*}p < 0.05$. Error bars are mean ± SEM.

Results

Multitrial training extends early odor preference memory to 48 h

We tested whether multitrial odor training could prolong odor memory compared with that induced by one-trial training. Training effects were significant among groups ($F_{(5,75)} = 2.675$, $p = 0.028$; Fig. 1). Pups that received a single day of odor conditioning (O/S$^+$) spent a greater proportion of time over peppermint-scented bedding (59.08 ± 6.94%, $n = 9$) compared with odor O/S$^-$ animals (32.76 ± 6.42%, $n = 9$) when tested 24 h later (*post hoc* Fisher: $t = 2.809$, $p = 0.006$). These differences were not apparent 48 h following training (O/S$^+$: 39.24 ± 4.88%, $n = 18$; O/S$^-$: 42.45 ± 5.07%, $n = 15$; $t = 0.463$, $p = 0.645$). The multiday O/S$^+$ group (52.33 ± 5.67%, $n = 13$), tested at 48 h, spent more time over peppermint than their O/S$^-$ counterparts (36.96 ± 4.50%, $n = 17$; $t = 2.100$, $p = 0.039$).

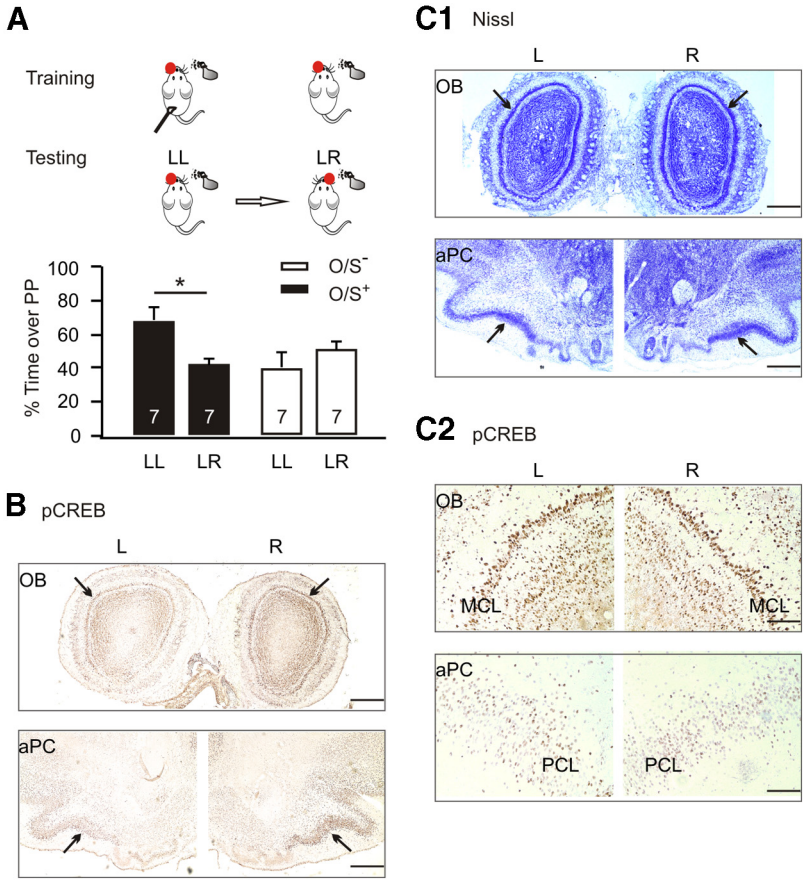

Figure 2. Lateralized learning is induced by single naris occlusion. ***A***, Percentage of time spent over peppermint-scented bedding among different groups in a two-choice test. The behavioral protocol is shown at the top. O/S$^+$ or O/S$^-$ animals with single naris occluded during training underwent odor preference testing, first with the same naris occluded and then with the opposite naris occluded. $^{*}p < 0.05$. Error bars are mean ± SEM. ***B***, pCREB expression in the occluded (L) and the spared (R) hemispheres following peppermint exposure in a single-naris-occluded pup. Arrows indicate mitral cell layer in the olfactory bulb (OB) and pyramidal cell layer (PCL) in the aPC. Scale bars, 500 μm. ***C1***, ***C2***, Assessment of tissue integrity and cell functioning following multiday reversible naris occlusions. ***C1***, Nissl staining of the olfactory bulb and aPC. Arrows indicate mitral cell layer (MCL) and pyramidal cell layer. Scale bars, 500 μm. ***C2***, pCREB staining of the corresponding areas indicated by arrows in ***C1***, under higher magnifications. Scale bars, 100 μm.

Synaptic changes at the LOT synapses parallel behaviorally detectable memory

We first established an intra-animal control protocol to assess synaptic changes in two hemispheres in the same animals. Before PD10, pups with single naris occlusion have access only to unilaterally stored olfactory information (Kucharski and Hall, 1987, 1988; Yuan and Harley, 2012). We confirmed that learning can be confined to one hemisphere via single naris occlusion following multitrial training. Pups who underwent O/S$^+$ training with left nostril occlusions spent significantly more time over peppermint when tested with the left nostril occluded (68.03 ± 8.45) than when tested with the right nostril occluded (42.00 ± 3.61; $n = 7$; $t = 2.593$, $p = 0.041$). While O/S$^-$ pups did not behave differently when tested with either the left (40.58 ± 8.46) or the right (50.88 ± 5.37; $n = 7$; $t = 1.055$, $p = 0.332$; Fig. 2*A*) nostril occluded. Significantly greater olfactory bulb and aPC pCREB staining was seen in the spared than occluded hemispheres, confirming lateralized odor activation ($n = 3$; Fig. 2*B*).

Multiday, short-term (~15 min), reversible naris occlusion did not visibly cause cell loss (see Nissl staining image, Fig. 2*C1*) or affect odor responsiveness (see pCREB image, Fig. 2*C2*) in either structure. Quantification of pCREB staining in both structures showed no differences in the spared versus occluded hemispheres (olfactory bulb: 0.072 ± 0.018 (occluded) vs 0.071 ± 0.014 (spared); aPC: 0.047 ± 0.006 (occluded) vs 0.035 ± 0.002 (spared); $p > 0.05$, $n = 4$). Taken together with behavioral results (Fig. 2*A*), this establishes a novel spaced training intra-animal model for the evaluation of synaptic changes.

Synaptic changes paralleled behavioral memory. In the single-trial O/S$^+$ group at 48 h, there was no difference in the

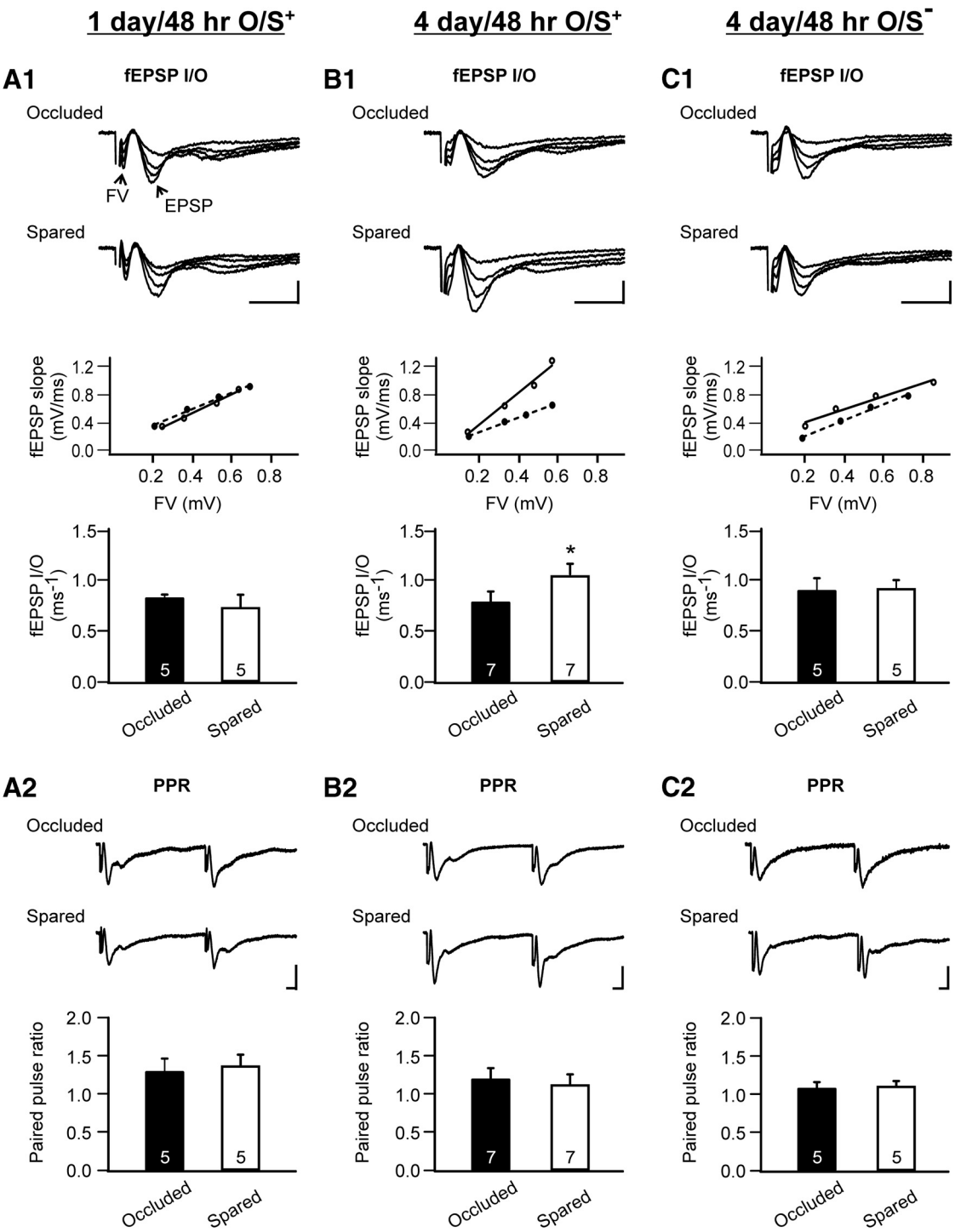

Figure 3. Learning induces LTP-like changes at the LOT to pyramidal cell synapse. ***A1***, ***A2***, I/O relationships and PPRs at the LOT synapses in the piriform cortex 48 h after 1 d O/S $^{+}$ training. Recordings from occluded and spared slices of the same animals were compared. ***A1***, Top, Examples of fEPSP traces at various stimulation intensities in an occluded and a spared slice from the same animal. Middle, I/O relationship of the slopes of the EPSPs and the sizes of the presynaptic volleys (FVs) from these two slices. Bottom, Average I/O from the two groups. ***A2***, Top, Example traces of paired-pulse recordings from an occluded and a spared slice from the same animal. Bottom, Average PPRs of the two groups. ***B1***, ***B2***, I/Os and PPRs of fEPSPs in the piriform cortex 48 h after multiday O/S $^{+}$ training. ***C1***, ***C2***, I/O and PPRs of fEPSPs in the piriform cortex 48 h after multiday O/S $^{-}$ training. Scale bars, 0.5 mV/5 ms. *$p < 0.05$. Error bars, mean ± SEM.

I/Os between the spared (0.82 ± 0.04) and occluded (0.74 ± 0.11) hemispheres ($t = 0.934$, $p = 0.403$, $n = 5$; Fig. 3*A1*), corresponding to no odor preference memory at 48 h (Fig. 1). The PPRs for the spared (1.31 ± 0.15) versus occluded (1.38 ± 0.14) hemispheres were not different either ($t = 0.538$, $p = 0.619$, $n = 5$; Fig. 3*A2*). However, in the multiday O/S $^{+}$ group, the I/O value for the spared hemisphere (1.08 ± 0.12) was significantly greater than that of the occluded hemisphere (0.81 ± 0.11; $t = 2.566$, $p = 0.043$, $n = 7$; Fig. 3*B1*). The PPRs for the spared (1.21 ± 0.13) versus occluded (1.13 ± 0.12) hemispheres were not different ($t = 1.025$, $p = 0.345$, $n = 7$; Fig. 3*B2*). In the control O/S $^{-}$ group, no significant differences were detected in either I/O values ($t = 0.212$, $p = 0.842$, $n = 5$; Fig. 3*C1*) or PPRs ($t = 0.157$, $p = 0.883$, $n = 5$; Fig. 3*C2*)

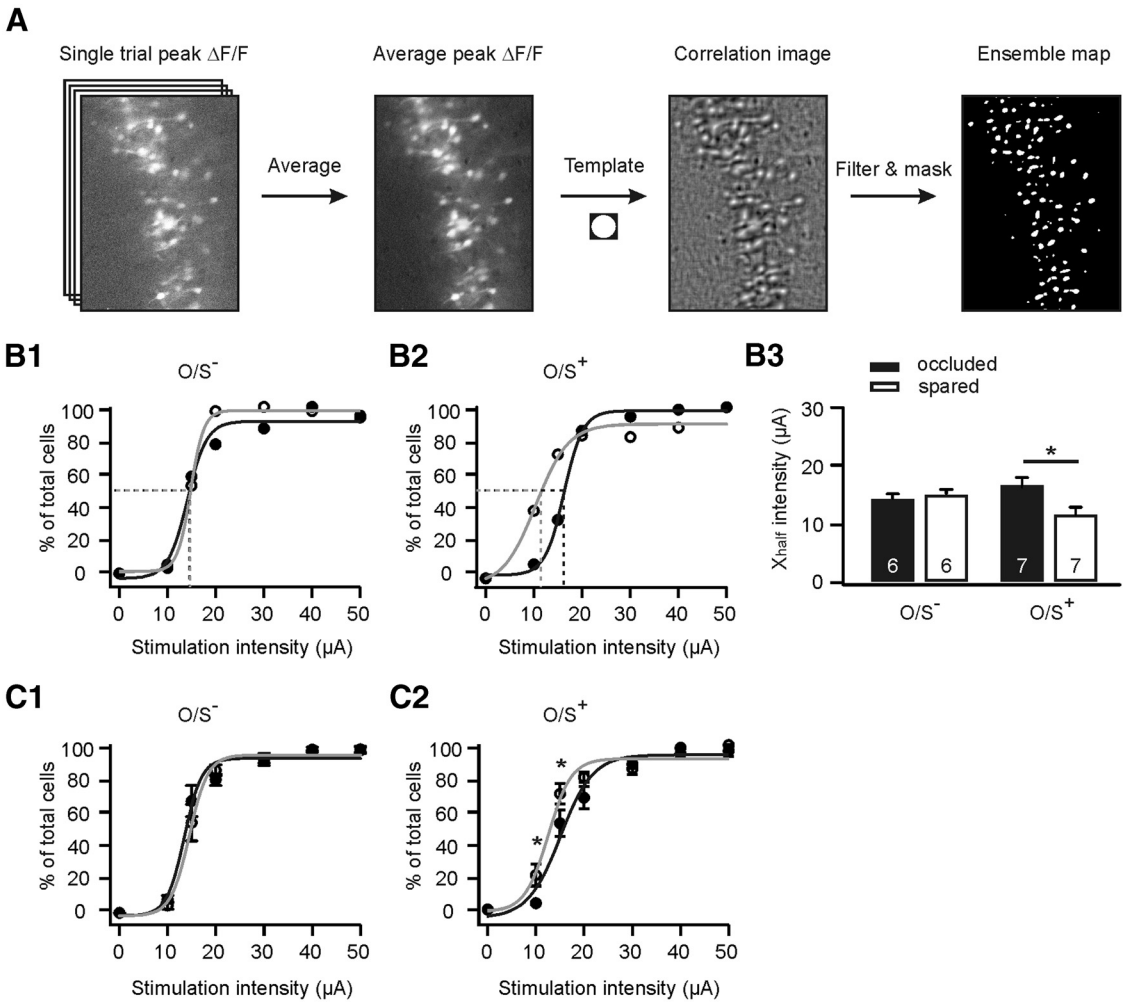

Figure 4. Learning results in enhanced pyramidal cell responses to perithreshold LOT stimulations. ***A***, Steps diagramming methods used to construct activity maps of cell ensembles. ***B1***, ***B2***, I/O relationships showing percentages of activated cells at various stimulation intensities from two hemispheres of the same animals. Closed circles indicate data from the occluded hemispheres; open circles are data from the spared hemispheres. ***B3***, Comparison of the half maximum activation intensities in the occluded and spared hemispheres in the O/S $^+$ and O/S $^-$ groups. ***C1***, ***C2***, Averaged I/O relationships in the O/S $^+$ and O/S $^-$ groups. Data are fit with sigmoid curves. *$p < 0.05$. Error bars are mean ± SEM.

between spared and occluded hemispheres. This result excludes the possibility that the synaptic changes seen in the multiday O/S $^+$ group are due to repeated odor exposure alone. Multiday odor conditioning results in a steeper I/O relationship that is most likely caused by postsynaptic changes such as increased AMPAR insertions (Franks and Isaacson, 2005; Morrison et al., 2013).

Multitrial odor training enhances pyramidal cell responses to LOT input

We tested whether the pyramidal cell firing properties are altered by odor training. While in the O/S $^-$ group, the X_{halfs} were comparable between the occluded (14.44 ± 0.67 μA) and spared (15.20 ± 0.85 μA) hemispheres ($t = 0.668$, $p = 0.534$, $n = 6$; Fig. 4*B1*,*B3*), in the O/S $^+$ group, the X_{half} was significantly lower in the spared hemisphere (11.53 ± 1.28 μA) than the occluded hemisphere (16.71 ± 1.26 μA; $t = 0.2.858$, $p = 0.029$, $n = 7$, Fig. 4*B2*,*B3*). The averaged I/O relationships in both groups are shown in Figure 4, *C1* (O/S $^-$) and *C2* (O/S $^+$). The left shift of the I/O curve in the O/S $^+$ group was caused by an increase in activated cells (%) at perithreshold stimulations (10 and 15 μA) in the spared hemispheres (Fig. 4*C2*). For example, at 10 μA stimulation intensity, 20.98 ± 6.61% cells were activated in the spared hemisphere, compared with 4.48 ± 1.60% activated cells in the occluded hemisphere ($t = 2.950$, $p = 0.012$, $n = 7$; Fig. 4*C2*). At 15 μA stimulation intensity, 70.30 ± 6.06% cells were activated in the spared hemisphere, compared with 52.30 ± 8.00% activated cells in the occluded hemisphere ($t = 2.182$, $p = 0.047$, $n = 5$; Fig. 4*C2*). While at the higher intensities (≥ 20 μA) in the O/S $^+$ group and at all intensities in the O/S $^-$ group, there were no differences in the percentages of activated cells in the spared versus occluded hemispheres (Fig. 4*C1*,*C2*). The total cell numbers activated are comparable in both O/S $^+$ group (occluded: 74.71 ± 7.41; spared: 82.57 ± 10.69; $t = 0.474$, $p = 0.652$, $n = 7$) and O/S $^-$ group (occluded: 68.00 ± 3.34; spared: 73.50 ± 9.62; $t = 0.626$, $p = 0.559$, $n = 6$). Together, these results suggest early odor preference learning induces synaptic potentiation at the LOT to pyramidal cell synapse in the aPC, bringing pyramidal cells closer to the threshold for firing and likely increasing the responsiveness of weakly activated cells to the CS odor. The calcium protocol used here does not evaluate spiking rate changes in cells already in the network but does reveal additional cell recruitment.

Discussion

These results are consistent with the canonical view that increases in synaptic strength underlie memory. They also suggest that in this cortical system, the learning-induced potentiation of the LOT fEPSP translates into a larger network response to odor input since previously weakly activated cells are likely recruited to participate in odor encoding. While synaptic AMPAR potentiation has previously been shown to support odor memory (Cui et al., 2011; Lethbridge et al., 2012; Yuan and Harley, 2012; Morrison et al., 2013), increases in aPC pyramidal cell excitability occur in adult rat odor discrimination rule learning (Saar and Barkai, 2003) and excitability changes could contribute to the altered network. Other inputs may also be modulated with learning. Hasselmo and colleagues (Linster and Hasselmo, 2001; Giocomo and Hasselmo, 2007) have reported cholinergic-induced synaptic changes in piriform associational connections.

This study confirms earlier findings of lateralized odor learning (Kucharski and Hall, 1987, 1988; Yuan and Harley, 2012) before the development of commissural fibers. Kucharski and Hall (1987, 1988) demonstrated that lateralized early memory spontaneously transfers to untrained cortex after PD11 and supports behavioral choice, providing evidence of dynamic memory reorganization in the piriform cortex.

Eight day training protocols (PD1–PD8) can produce memory at PD19 (Woo and Leon, 1987). The present multitrial memory may also extend beyond 48 h. The increase in AMPAR responses and the larger aPC network could now be examined over a range of memory durations.

The lateralized odor preference model also permits us to ask whether memory strength relates to the strength of synaptic change. For each pup, we derived a preference measure for the trained and untrained nares. The relative synaptic difference may index learning strength. Subsequent physiological experiments might provide correlative insights into the relation of those synaptic and network changes to memory expression.

References

Apicella A, Yuan Q, Scanziani M, Isaacson JS (2010) Pyramidal cells in piriform cortex receive convergent input from distinct olfactory bulb glomeruli. J Neurosci 30:14255–14260. CrossRef Medline

Christie-Fougere MM, Darby-King A, Harley CW, McLean JH (2009) Calcineurin inhibition eliminates the normal inverted U curve, enhances acquisition and prolongs memory in a mammalian 3′-5′-cAMP-dependent learning paradigm. Neuroscience 158:1277–1283. CrossRef Medline

Cui W, Darby-King A, Grimes MT, Howland JG, Wang YT, McLean JH, Harley CW (2011) Odor preference learning and memory modify GluA1 phosphorylation and GluA1 distribution in the neonate rat olfactory bulb: testing the AMPA receptor hypothesis in an appetitive learning model. Learn Mem 18:283–291. CrossRef Medline

Cummings DM, Henning HE, Brunjes PC (1997) Olfactory bulb recovery after early sensory deprivation. J Neurosci 17:7433–7440. Medline

Fillion TJ, Blass EM (1986) Infantile experience with suckling odors determines adult sexual behavior in male rats. Science 231:729–731. CrossRef Medline

Franks KM, Isaacson JS (2005) Synapse-specific downregulation of NMDA receptors by early experience: a critical period for plasticity of sensory input to olfactory cortex. Neuron 47:101–114. CrossRef Medline

Giocomo LM, Hasselmo ME (2007) Neuromodulation by glutamate and acetylcholine can change circuit dynamics by regulating the relative influence of afferent input and excitatory feedback. Mol Neurobiol 36:184–200. CrossRef Medline

Kucharski D, Hall WG (1987) New routes to early memories. Science 238:786–788. CrossRef Medline

Kucharski D, Hall WG (1988) Developmental change in the access to olfactory memories. Behav Neurosci 102:340–348. CrossRef Medline

Lethbridge R, Hou Q, Harley CW, Yuan Q (2012) Olfactory bulb glomerular NMDA receptors mediate olfactory nerve potentiation and odor preference learning in the neonate rat. PLoS One 7:e35024. CrossRef Medline

Linster C, Hasselmo ME (2001) Neuromodulation and the functional dynamics of piriform cortex. Chem Senses 26:585–594. CrossRef Medline

Malenka RC, Bear MF (2004) LTP and LTD: an embarrassment of riches. Neuron 44:5–21. CrossRef Medline

Matsuo N, Reijmers L, Mayford M (2008) Spine-type-specific recruitment of newly synthesized AMPA receptors with learning. Science 319:1104–1107. CrossRef Medline

McLean JH, Smith A, Rogers S, Clarke K, Darby-King A, Harley CW (2009) A phosphodiesterase inhibitor, cilomilast, enhances cAMP activity to restore conditioned odor preference memory after serotonergic depletion in the neonate rat. Neurobiol Learn Mem 92:63–69. CrossRef Medline

Morrison GL, Fontaine CJ, Harley CW, Yuan Q (2013) A role for the anterior piriform cortex in early odor preference learning: evidence for multiple olfactory learning structures in the rat pup. J Neurophysiol 110:141–152. CrossRef Medline

Raineki C, Shionoya K, Sander K, Sullivan RM (2009) Ontogeny of odor-LiCl vs odor-shock learning: similar behaviors but divergent ages of functional amygdala emergence. Learn Mem 16:114–121. CrossRef Medline

Roth TL, Sullivan RM (2005) Memory of early maltreatment: neonatal behavioral and neural correlates of maternal maltreatment within the context of classical conditioning. Biol Psychiatry 57:823–831. CrossRef Medline

Saar D, Barkai E (2003) Long-term modifications in intrinsic neuronal properties and rule learning in rats. Eur J Neurosci 17:2727–2734. CrossRef Medline

Schwob JE, Price JL (1984) The development of axonal connections in the central olfactory system of rats. J Comp Neurol 223:177–202. CrossRef Medline

Whitlock JR, Heynen AJ, Shuler MG, Bear MF (2006) Learning induces long-term potentiation in the hippocampus. Science 313:1093–1097. CrossRef Medline

Woo CC, Leon M (1987) Sensitive period for neural and behavioral response development to learned odors. Brain Res 433:309–313. Medline

Yuan Q, Harley CW (2012) What a nostril knows: olfactory nerve-evoked AMPA responses increase while NMDA responses decrease at 24 h post-training for lateralized odor preference memory in neonate rat. Learn Mem 19:50–53. CrossRef Medline

Yuan Q, Isaacson JS, Scanziani M (2011) Linking neuronal ensembles by associative synaptic plasticity. PLoS One 6:e20486. CrossRef Medline